ELSEVIER

Journal of Molecular Catalysis A: Chemical 174 (2001) 141–149

JOURNAL OF MOLECULAR CATALYSIS A: CHEMICAL

www.elsevier.com/locate/molcata

Homogeneous hydrogenation of imines catalyzed by rhodium and iridium complexes Kinetics and mechanism of the hydrogenation of *N*-(β-naphthyl methylene) aniline using $[Ir(COD)(PPh_3)_2]PF_6$ as catalyst precursor

V. Herrera [a,*], B. Muñoz [a], V. Landaeta [a], N. Canudas [b]

[a] *Centro de Química, Instituto Venezolano de Investigaciones Científicas (IVIC), Caracas 1020-A, Venezuela*
[b] *Departamento de Química, Universidad Simón Bolívar, Valle de Sartenejas, Estado Miranda, Venezuela*

Received 23 January 2001; received in revised form 26 April 2001; accepted 26 April 2001

Abstract

The regioselective hydrogenation of some imines to the corresponding amines is efficiently catalyzed by $[Ir(COD)(PPh_3)_2]PF_6$ (**1**) and $[Rh(COD)(PPh_3)_2]PF_6$ (**2**) at 60°C and 200 psi of H_2. The kinetics of the hydrogenation of *N*-(β-naphthyl methylene) aniline (NβNA) with $[Ir(COD)(PPh_3)_2]PF_6$ in tetrahydrofuran (THF) have been studied. The experimentally determined rate law is $r_i = k_{cat}[Ir][N\beta NA][H_2]$ where $k_{cat} = (2.2 \pm 0.3) \times 10^3\ M^{-2}\ s^{-1}$ at 323 K and the corresponding activation parameters are: $\Delta H^\circ = (4.0 \pm 0.4)$ kcal mol^{-1}; $\Delta S^\circ = (-32 \pm 2)$ e.u.; $\Delta G^\circ = (14 \pm 2)$ kcal mol^{-1}. A catalytic cycle is proposed on the basis of the kinetic experiments and some NMR data.

Keywords: Hydrogenation of imines; Homogeneous catalysis; Iridium; Rhodium; Kinetics; Mechanism

1. Introduction

The catalytic hydrogenation of imines to amines has attracted considerable interest in recent years, for simple substrates and for prochiral ones [1–8]. Homogeneous hydrogenation of carbon–nitrogen double bonds, though more difficult and consequently less developed than the corresponding reduction of carbon–carbon and carbon–oxygen double bonds, has been the focus of much recent attention [9]. This reaction that produces the corresponding amine under mild conditions is important for organic synthesis and in the literature we found that drastic conditions are needed for a complete hydrogenation (40–50°C and 20–30 atm gas pressure). In homogeneous systems, only a few catalysts are effective for aldimine and ketimine [10,11] reduction but they are mostly, if not all, also effective for alkene and/or ketone hydrogenation.

Most attention has been focused on iridium complexes and previous studies from our laboratory [12–17] have demonstrated that the complexes $[Ir(COD)(PPh_3)_2]PF_6$ (**1**) and $[Rh(COD)(PPh_3)_2]PF_6$ (**2**) are useful catalysts for a variety of hydrogenation reactions.

* Corresponding author. Tel.: +58-212-5041307; fax: +58-212-5041775/5041350.
E-mail address: vherrera@quimica.ivic.ve (V. Herrera).

1381-1169/01/$ – see front matter
PII: S1381-1169(01)00197-2

Herein we report a comparison between complexes **1** and **2** as catalytic precursors in the hydrogenation of imines and a kinetic and mechanistic study of the most effective system found.

2. Experimental

2.1. General procedures

All reactions and manipulations were routinely performed under a nitrogen atmosphere by using standard Schlenck techniques. Solvents of analytical grade were distilled from the appropriate drying agents under N_2 immediately prior to use. Aniline (Aldrich) was purified by reduced pressure distillation. Hydrogen was purified through two columns in series containing CuO/Al_2O_3 and $CaSO_4$, respectively. Tetrahydrofuran (THF) was distilled from sodium/benzophenone, methanol from $CaSO_4$ and dichlorometane from P_2O_5. All of the imines were synthesized according to the method reported in [18]. All other chemicals were commercial products and were used as received without further purification. Literature methods were employed for the synthesis of $[Ir(COD)Cl]_2$ [19], **1** [20], $[Rh(COD)Cl]_2$ [21], **2** [22], and $[Ir(H)_2(Me_2CO)_2(PPh_3)_2]PF_6$ [23].

2.2. Physical measurements

Infrared spectra were recorded on a Nicolet-FTIR Magna 590 spectrometer using samples in KBr disk. Deuterated solvents for NMR measurements were dried over molecular sieves. ^1H, $^{13}C\{^1H\}$ and $^{31}P\{^1H\}$ NMR spectra were obtained on a Bruker AM-300 (300 MHz) spectrometer. ^1H NMR shifts are recorded relative to the residual ^1H resonance in the deuterated solvent. Gas chromatograph (GC)–MS analyses were performed on a HP-5890 GC equipped with a mass selective detector HP-5972 and a Carbowax capillary column. Reactions under controlled pressure of hydrogen were performed with a Parr reactor.

3. Catalytic hydrogenation of imines

3.1. Parr reactor experiments

In a typical experiment a solution of the catalyst precursor and a 100-fold excess of the imine in THF (or methanol, or CH_2Cl_2) (5 ml) were placed into the Parr reactor. After introduction of the catalysis components, the reactor was flushed with H_2 to remove oxygen and then pressurized to the desired pressure at room temperature, heated to the appropriate temperature, and immediately stirred. After 18 h, the reactor was cooled to room temperature and slowly depressurized. A sample of the solution was withdrawn and analyzed by GC–MS. The reaction conditions and the results of these experiments have been collected in Table 1.

3.2. Kinetic measurements

In a typical experiment, a solution of the catalyst $[Ir(COD)(PPh_3)_2]PF_6$ and the substrate in THF was placed in a glass reactor fitted with a reflux condenser kept at $-5^\circ C$. The reactor was sealed with Apiezon wax to a high-vacuum line, and the solution was carefully degassed by three freeze–pump–thaw cycles; hydrogen was admitted at this point to the desired pressure, an electric oven preheated to the required temperature was placed around the reactor, and magnetic stirring was immediately turned on. The reaction was followed by measuring the hydrogen pressure drop as a function of time. Each run was repeated at least twice to ensure reproducibility of the results.

The conversion of reactants in the catalytic reactions was generally (although not necessarily) kept below 10% in order to use the initial rates method in our calculations. The measured $\Delta P(H_2)$ values were converted to mmol of amine produced, and the data were plotted as molar concentration of the product as a function of time, yielding straight lines. Initial rates were then obtained from the corresponding slopes. All the straight lines were fitted by use of conventional linear regression software to $r^2 > 0.98$. Concentrations of dissolved hydrogen were calculated using published solubility data [24].

3.3. NMR experiments

A 5 mm NMR tube was charged with a solution of $[Ir(H)_2(Me_2CO)_2(PPh_3)_2]PF_6$ (15 mg; 0.0153 mmol) in acetone-d_6 (0.5 ml) under nitrogen. The tube was cooled at $-80^\circ C$, the *N*-(β-naphthyl methylene) aniline (NβNA) was added (35 mg; 0.153 mmol) and then

Table 1
Hydrogenation of imines catalyzed by iridium and rhodium complexes after 18 h at 200 psi H_2 initial pressure

Entry	Substrate	Catalyst	T (°C)	Yield (%)
1	**A**	**1**	60	0
			100	60
		2	60	0
			100	80
2	**B**	**1**	25	87
			60	96
			100	93
		2	25	87
			60	87
			100	90
3	**C**	**1**	60	0
			100	95
		2	60	0
			100	70
4	**D**	**1**	60	90
			100	98
		2	60	82
			100	89
5	**E**	**1**	60	10
			100	90
		2	60	2
			100	88
6	**F**	**1**	60	5
			100	80
		2	60	0
			100	60
7	**G**	**1**	60	0
			100	100
		2	60	0
			100	60

placed into a NMR probe at the same temperature. The reaction was followed by variable-temperature $^{31}P\{^1H\}$ and ^1H NMR spectroscopy over the range of −80 to +40°C.

4. Results and discussion

4.1. Autoclave reactions

The imines shown in Scheme 1 are efficiently hydrogenated to the corresponding amines catalyzed by **1** and **2** under mild conditions (Table 1). The effect of temperature on the conversion to the amine was investigated. At 100°C and 200 psi of H_2, all of the imines selected are reduced by Ir complex over 60%. The rhodium system was less efficient but in some cases it reduces with high conversion rates too. At 60°C and the same pressure there is no significant difference in amine yields for the reduction of imines **B** and **D** for both catalysts. These imines are structurally similar, having a minimal steric hindrance around the C=N moiety, making the hydrogenation reaction easier, like an olefin hydrogenation. While the reduction in these two cases occurs with mild conditions, all of the other cases need higher temperatures to obtain good yields of the corresponding amine. In the particular case of the hydrogenation of NβNA (**B**) catalyzed by **1**, we found that at 60°C and 200 psi of H_2, a conversion of 96% was achieved. Then, these results would indicate that the rate of C=N moieties reduction decreases with increasing steric hindrance around them, demonstrating that this effect plays an important role in the reduction of C=N double bonds.

4.2. Kinetic studies

The kinetics of the hydrogenation of NβNA to the corresponding amine (Eq. (1)) was studied in

Table 2
Kinetic data for the hydrogenation of NβNA with **1** as the catalyst precursor

10^4[Ir] (M)	10^2[NβNA] (M)	10^5[H_2] (M)	T (°C)	$10^6 r_i$ (M s^{-1})
4.0	2.5	7.36	323	1.7 ± 0.1
5.0	2.5	7.36	323	2.2 ± 0.3
6.0	2.5	7.36	323	2.5 ± 0.3
7.0	2.5	7.36	323	2.9 ± 0.8
7.7	2.5	7.36	323	3.0 ± 1.0
5.0	1.5	7.36	323	1.0 ± 0.3
5.0	3.5	7.36	323	2.9 ± 0.6
5.0	4.5	7.36	323	3.8 ± 0.4
5.0	5.5	7.36	323	4.2 ± 0.3
5.0	2.5	5.28	323	1.5 ± 0.1
5.0	2.5	6.29	323	2.0 ± 0.2
5.0	2.5	8.17	323	2.5 ± 0.3
5.0	2.5	7.36	309	1.5 ± 0.6
5.0	2.5	7.36	330	2.4 ± 0.3
5.0	2.5	7.36	333	2.5 ± 0.1
5.0	2.5	7.36	341	3.0 ± 0.9

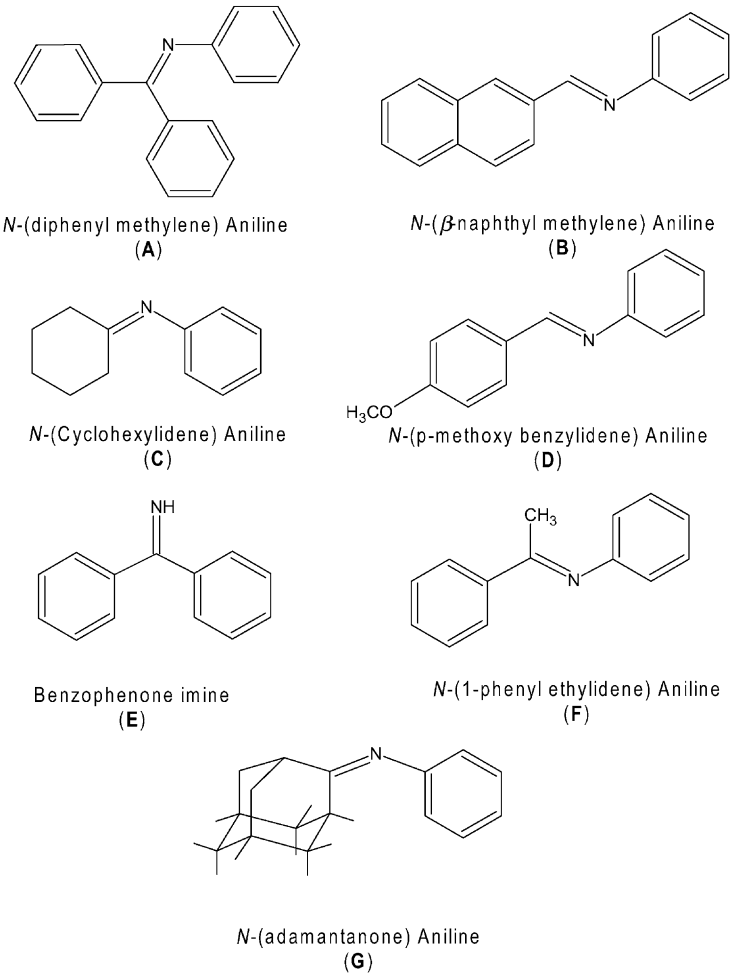

Scheme 1.

THF by carrying out runs at different catalyst, substrate and hydrogen concentrations and at different temperatures. The complete data are listed in Table 2.

The concentration of complex **1** was varied from 4×10^{-4} to 7.7×10^{-4} M while the amine and dissolved hydrogen concentrations (2.5×10^{-2} and 7.36×10^{-5} M, respectively), and the temperature (323 K) were kept constant. The initial rates of hydrogenation of NβNA (r_i) showed a direct dependence with

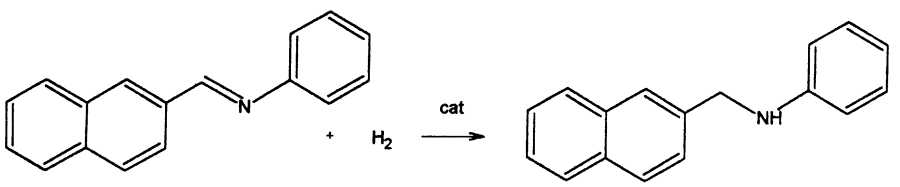

(1)

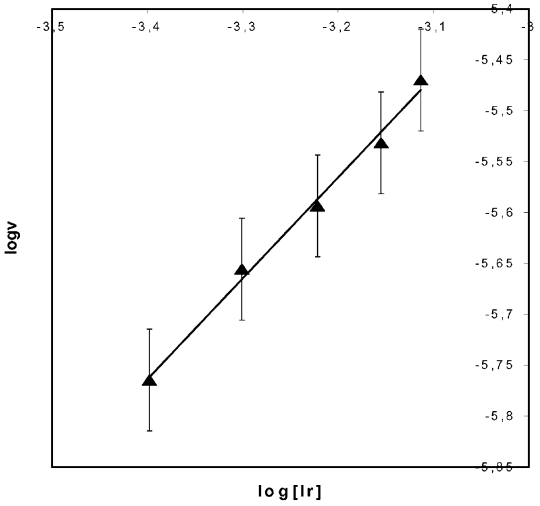

Fig. 1. Rate dependence of *N*-(β-naphthyl methylene) aniline hydrogenation with respect to catalyst concentration.

respect to the catalyst concentration. The plot of $\log r_i$ versus log[Ir] (Fig. 1) yields a straight line of slope 0.99, which confirms the first-order dependence.

The effect of NβNA concentration on the reaction rate was studied varying from 1.5×10^{-2} to 5.5×10^{-2} M, keeping the iridium and dissolved hydrogen concentration and temperature constant. Fig. 2 shows a first-order dependence of the hydrogenation

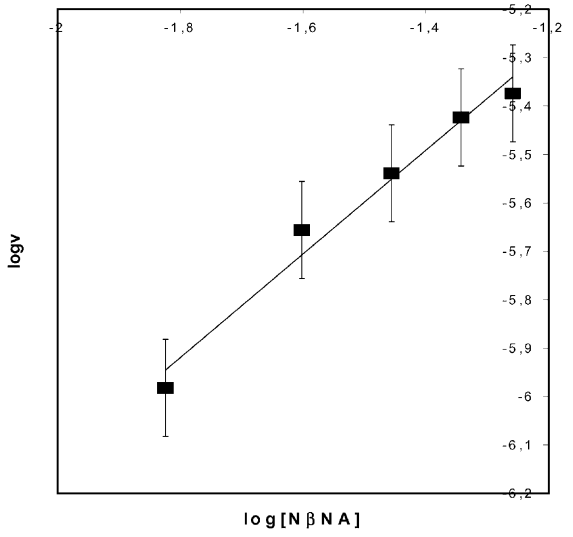

Fig. 2. Rate dependence of *N*-(β-naphthyl methylene) aniline hydrogenation with respect to substrate concentration.

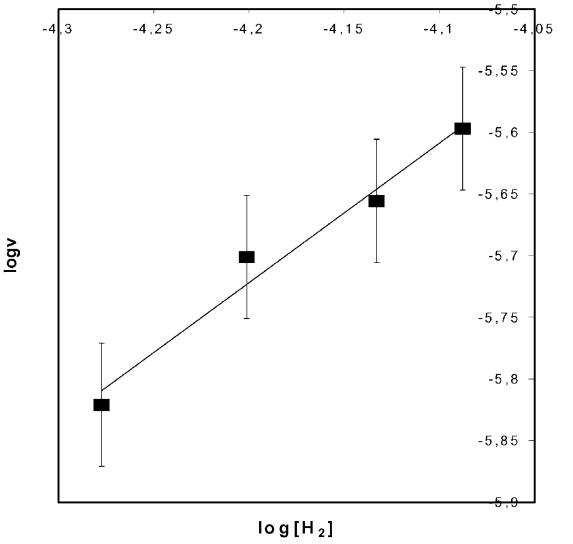

Fig. 3. Rate dependence of *N*-(β-naphthyl methylene) aniline hydrogenation with respect to hydrogen concentration.

rate with respect to substrate concentration (the slope value of the plot $\log r_i$ versus log[NβNA] = 1.07). The variation of the initial rates with hydrogen concentration indicates a first-order dependence at low pressures. This first-order dependence was confirmed by the slope value of plot $\log r_i$ versus $\log[H_2]$ (slope = 1.13) (Fig. 3). Consequently, the experimental rate law can be written as

$$r_i = k_{cat}[Ir][H_2][N\beta NA] \quad (2)$$

Eq. (2) allowed us to calculate an experimental value for the catalytic rate constant at 50°C [$k_{cat} = (2.2 \pm 0.3) \times 10^3\ M^{-2}\ s^{-1}$].

The effect of the temperature on the rate constant was studied in the range 309–341 K for concentrations of NβNA at 2.5×10^{-2} M, catalyst at 5.0×10^{-4} M, and dissolved hydrogen at 7.36×10^{-5} M. Within the range of conditions used, the variation of the solubility of hydrogen with temperature is negligible. A plot of $\ln k_{cat}$ versus $1/T$ (Fig. 4) allowed us to evaluate the activation energy E_a, the frequency factor A, the extrapolated value of the rate constant at 298 K, and the values of enthalpy, entropy and free energy of activation (calculated from the equations $\Delta H^\circ = E_a - RT$, $\Delta S^\circ = R \ln(hA/e^2 k_B T)$, and $\Delta G^\circ = \Delta H^\circ - T\,\Delta S^\circ$); these values are listed in Table 3.

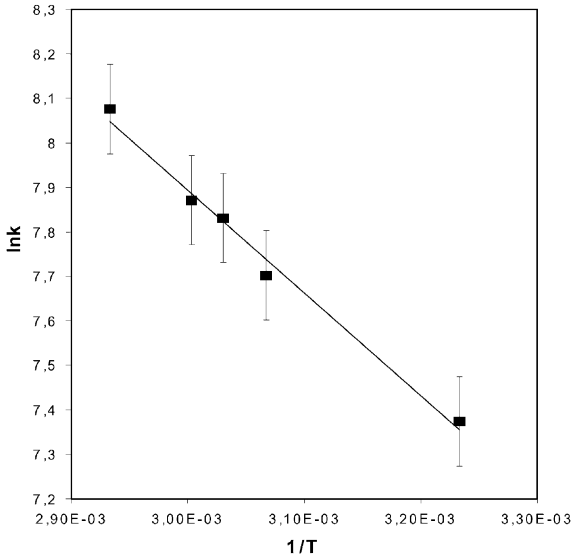

Fig. 4. Effect of temperature on the *N*-(β-naphthyl methylene) aniline hydrogenation rate.

The effect of the solvent on the kinetic reactions was investigated using 1,2-dichloroethane, THF, dichloromethane and acetone. As we can observe in Fig. 5, the catalytic rates decrease with the coordinating capacity of the solvent: the poorly coordinating 1,2-dichloroethane results in the higher hydrogenation rate, followed by THF and dichloromethane, and the stronger coordinating acetone inhibits the catalysis. We presume that this effect would indicate the presence of the coordinatively unsaturated species within the kinetically important catalytic cycle, and these species are probably stabilized through coordination of solvent molecules in a competition of these with the substrate for the vacant coordination sites.

Table 3
Activation parameters for the hydrogenation of NβNA with **1** as the catalyst precursor

E_a (kcal mol^{-1})	4.6 ± 0.4
A (M^{-2} s^{-1})	(3.0 ± 1.0) × 10^6
k_{cat} (25°C) (M^{-2} s^{-1})	1178.45
ΔH° (kcal mol^{-1})	4.0 ± 0.4
ΔS° (e.u.)	−33 ± 2
ΔG° (kcal mol^{-1})	14 ± 2

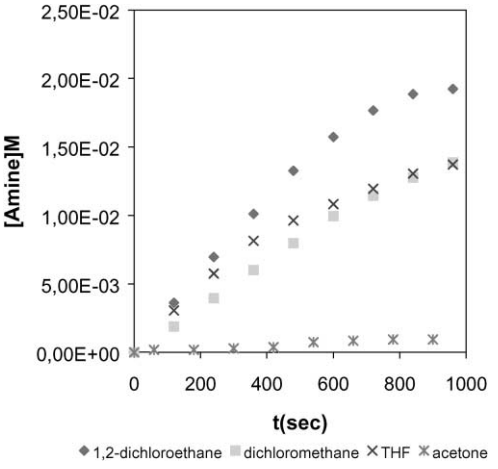

Fig. 5. Effect of solvent on the *N*-(β-naphthyl methylene) aniline hydrogenation rate.

4.3. Coordination chemistry related to the hydrogenation of NβNA

In order to complement the kinetic study of the hydrogenation of NβNA, we have tried to establish some of the active species implicated in the catalysis. It is well known that complex **1** reacts with hydrogen in coordinating solvents to give a dihydridobis(solvento) complex $[Ir(H)_2(S)_2(PPh_3)_2]PF_6$ (S = solvent) (**3**) [23] (Eq. (3)).

$$\underset{\mathbf{1}}{[Ir(COD)(PPH_3)_2]PF_6} \xrightarrow[\text{Solvent}]{H_2} \underset{\mathbf{3}}{[Ir(H)_2(S)_2(PPh_3)_2]PF_6} \quad (3)$$

Complex **3** reacts with NβNA at −80°C to yield an equilibrium mixture of **3** plus two new complexes, which are presumably the mono- and di-substitution products $[Ir(H)_2(S)(N\beta NA)(PPh_3)_2]PF_6$ (**4**) and $[Ir(H)_2(N\beta NA)_2(PPh_3)_2]PF_6$ (**5**).

The high-field ^{1}H NMR spectra for **5** shows a triplet at −16.9 ppm (acetone-d_6, 300 MHz), while the corresponding $^{31}P\{^1H\}$ spectra consists of a singlet at 18.5 ppm. These features indicate the presence of two equivalent hydrides coupled with two equivalent phosphines, corresponding to a stereochemistry involving mutually *trans*-phosphines, and mutually *cis*-pairs of hydride and imine ligands. The high-field ^{1}H NMR spectra for **4** shows two triplets of doublets at −16.2 and −16.5 ppm (^2J(H–H) = 3 Hz,

Table 4
NMR data[a] (δ, ppm) for compounds **3–5** in acetone-d_6

Complex	^{1}H	^{31}P{^{1}H}
3	−27.3 (t)[b]	31.3 (s)
4	−16.2 (td)[b,c] −16.5 (td)	18.4 (s)
5	−16.9 (t)[b]	18.5 (s)

[a] At −80°C.
[b] J(H–P) = 15.8 Hz.
[c] ^2J(H–H) = 3 Hz.

and J(H–P) = 15.75 Hz) and the ^{31}P{^{1}H} spectrum consists of a singlet at 18.4 ppm, indicating that the two equivalent phosphines remain in *trans*-disposition and two different *cis*-hydrides are *trans* to an imine and solvent ligands. ^{1}H and ^{31}P{^{1}H} NMR data are contained in Table 4. It is interesting to note that all complexes prefer to adopt the more sterically crowded stereochemistry containing one or two *cis*-imines rather than an all *trans*-disposition of the six ligands, most probably as a result of the large *trans* effect typical of hydride ligands.

The results are summarized in Scheme 2.

4.4. Mechanism of NβNA hydrogenation

On the basis of the results presented above, we propose that under the conditions of the catalytic reaction, complex **1** reacts with hydrogen and solvent to give **3**, which is proposed as the initial species entering the catalytic cycle. Then, **3** coordinates one imine molecule to form **4** through the equilibrium K_1 shown in Eq. (4).

$$[\underset{\mathbf{3}}{Ir(H)_2(S)_2(PPh_3)_2}]PF_6 + N\beta NA \overset{K_1}{\rightleftharpoons} [\underset{\mathbf{4}}{Ir(H)_2(S)(N\beta NA)(PPh_3)_2}]PF_6 \quad (4)$$

The subsequent reaction of **4** to release the product amine and produce the unsaturated species $[Ir(S)_2(PPh_3)_2]PF_6$ (**6**) is the rate determining step as shown in Eq. (5).

$$[\underset{\mathbf{4}}{Ir(H)_2(S)(N\beta NA)(PPh_3)_2}]PF_6 \overset{k_2}{\rightarrow} [\underset{\mathbf{6}}{Ir(S)_2(PPh_3)_2}]PF_6 + \text{amine} \quad (5)$$

The catalytic cycle is completed with the oxidative addition of hydrogen to regenerate **3** (Eq. (6)).

$$[\underset{\mathbf{6}}{Ir(S)_2(PPh_3)_2}]PF_6 + \overset{K_4}{\rightleftharpoons} [\underset{\mathbf{3}}{Ir(H)_2(S)_2(PPh_3)_2}]PF_6 \quad (6)$$

A rate law corresponding to this mechanism can be derived, taking into account that the rate of amine production is

$$r = \frac{d[\text{amine}]}{dt} = k_2[4] \quad (7)$$

Considering the equilibrium showed in Eqs. (4) and (6), and the mass balance for iridium, and substituting [**4**] in Eq. (7), the rate expression becomes

$$r = \frac{k_2 K_1 K_4 [Ir]_0 [H_2][N\beta NA]}{1 + K_4[H_2] + K_1 K_4 [H_2][N\beta NA]} \quad (8)$$

Eq. (8) can be inverted and reorganized as

$$\frac{[Ir]_0[N\beta NA]}{r} = \frac{1}{k_2 K_1 K_4 [H_2]} + \frac{1 + K_1[N\beta NA]}{k_2 K_1} \quad (9)$$

A plot of the reciprocal of the rate of NβNA hydrogenation versus the reciprocal of hydrogen concentration yields a straight line from which the value of $k_2K_1K_4$ ($2.8 \times 10^3\ M^{-2}\ s^{-1}$) can be obtained. If the term $(K_4[H_2] + K_1K_4[H_2][N\beta NA]) \ll 1$ (Eq. (8)), the rate expression can be approximated to

$$r = k_2 K_1 K_4 [Ir]_0 [H_2][N\beta NA] \quad (10)$$

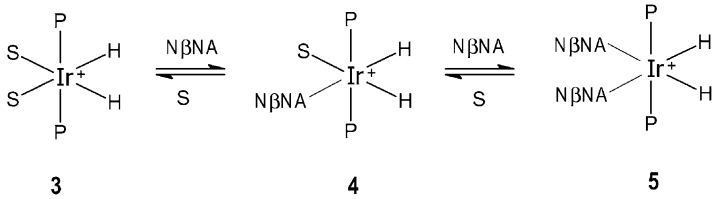

3 **4** **5**

Scheme 2.

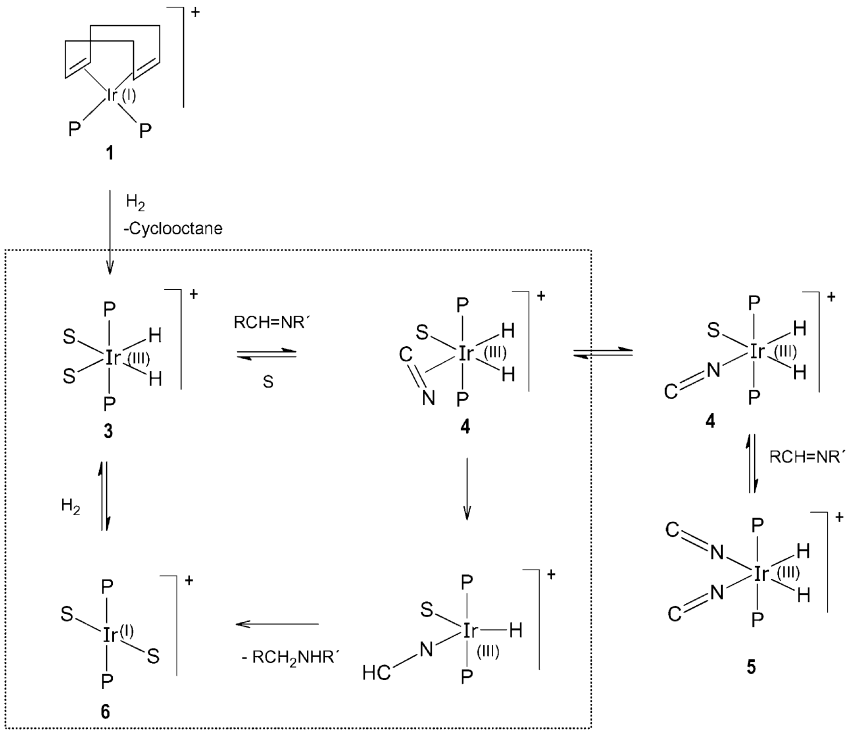

Scheme 3.

Which is identical to the experimental rate law $k_{cat} = k_2K_1K_4$ and the value of $k_2K_1K_4$ ($2.8 \times 10^3\,M^{-2}\,s^{-1}$) is in agreement with the experimental value obtained ($2.2 \times 10^3\,M^{-2}\,s^{-1}$).

Also, Eq. (8) can be reorganized again as

$$\frac{[Ir]_0[H_2]}{r} = \frac{1 + K_4[H_2]}{k_2K_1K_4[N\beta NA]} + \frac{[H_2]}{k_2} \qquad (11)$$

A plot of the reciprocal of the rate of NβNA hydrogenation versus the reciprocal of NβNA concentration yields a straight line in agreement with the kinetic results. From these plots the values of k_2 ($0.052\,s^{-1}$), K_1 ($22.14\,M^{-1}$) and K_4 ($2.4 \times 10^3\,M^{-1}$) can be obtained.

Although, the details of each step involved in the mechanism have not been elucidated, a general schematic cycle for the $[Ir(COD)(PPh_3)_2]PF_6$-catalyzed hydrogenation of NβNA is proposed (Scheme 3) in accordance with the experimentally determined rate law.

We believe that once complex **1** generates the species **3**, the incoming NβNA would occupy the sites *trans* to the hydride ligands to form the mono- and di-substitution products **4** and **5** (Scheme 2).

In the literature has been proposed that imines can coordinate in two different modes to the metal center [1]: by the nitrogen atom (η^1-N) or by the double bond C=N (η^2-N, C), where the η^2-bonding mode is more likely to occur in the hydrogenation reaction (Scheme 4). With the NMR data obtained we have not been able to distinguish how the imine is coordinated to the iridium center, but probably the

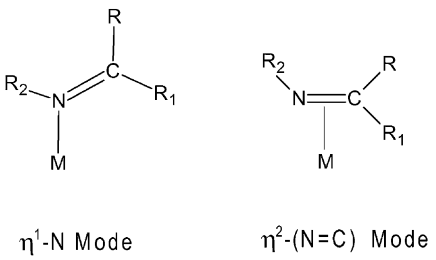

Scheme 4.

mono-coordinated species **4** corresponds to an equilibrium mixture of the two forms; where the η^1-N mode is out of the cycle and the η^2-bonding mode is the olefin-like intermediate that undergoes selective hydrogenation of the C=N bond (Scheme 3).

In our previous work, we proposed similar transformations in the mechanistic cycle for the hydrogenation of benzothiophene [14].

On the other hand, we propose that the complex **5** has both imines coordinated by the N-atom, because the η^2-(C=N)-imine coordination in a bis-imine complex would not be possible for steric reasons.

Then, the complex **4** would evolve by successive transfer the hydrides to the imine. Considering that Ir-hydrides generally have a very hydridic character, we presume that the first transfer will go to the carbon atom to yield the iridium-alkylaminium intermediate. Reductive elimination of the amine generates the unsaturated species $[Ir(S)_2(PPh_3)_2]PF_6$, which reacts with hydrogen to produce **3** and restart the cycle.

5. Conclusions

We have studied the hydrogenation of imines using rhodium and iridium complexes as catalyst precursors, finding that the iridium complex is the better catalyst precursor. The kinetic study of the hydrogenation of NβNA with **1** in THF was done and we have established the experimental rate law as $r_i = k_{cat}[Ir][H_2][N\beta NA]$, where $k_{cat} = (2.2 \pm 0.3) \times 10^3\,M^{-2}\,s^{-1}$. Besides, we have suggested a mechanistic scheme for this reaction, which is consistent with the kinetic and spectral data. The initial species entering the catalytic cycle is **3** and we proposed a rate determining step corresponding to the first hydride transfer.

Further work using similar iridium and rhodium complexes for kinetic and mechanistic studies for the same reaction are in progress, and some extensions of this work with prochiral imines are programmed to be done.

Acknowledgements

The authors are grateful to CONICIT for financial support (S1-95000693), to Dr. R. Sánchez-Delgado for his useful comments and suggestions, and Mr. A. Fuentes for his assistance in the experimental work.

References

[1] B.R. James, Catal. Today 12 (1997) 209.
[2] C.J. Longley, T. Goodwin, G. Wilkinson, Polyhedron 5 (1986) 1625.
[3] R.B. Bedford, P.A. Chaloner, C. Claver, E. Fernández, P.B. Hitchcock, A. Ruiz, Chem. Ind. 62 (1994) 181.
[4] A.G. Becalski, W.R. Cullen, M.D. Fryzuk, B.R. James, G.J. Kang, S.J. Rettig, Inorg. Chem. 30 (1991) 5002.
[5] W.R. Cullen, M.D. Fryzuk, B.R. James, J.P. Kutney, G.J. Kang, G. Herb, I.S. Thorburn, R. Spogliarich, J. Mol. Catal. 62 (1990) 243.
[6] N. Uematsu, A. Fujii, S. Hashiguchi, T. Ikariya, R. Noyori, J. Am. Chem. Soc. 118 (1996) 4916.
[7] Y.N. Cheong, J. Osborn, J. Am. Chem. Soc. 112 (1990) 9400.
[8] C.A. Willoughby, S.L. Buchwald, J. Am. Chem. Soc. 116 (1994) 8952, 11703
[9] B.R. James, G. Ball, W.R. Cullen, M.D. Fryzuk, W. Henderson, K. McFarlane, Inorg. Chem. 33 (1994) 1464.
[10] Y. Cheong, D. Meyer, J. Osborn, J. Chem. Soc. Chem. Commun. (1990) 869.
[11] J. Osborn, R. Sablong, Tetrahedron Lett. 37 (1996) 4937.
[12] C. Bianchini, A. Meli, M. Peruzzini, F. Vizza, P. Frediani, V. Herrera, R. Sánchez-Delgado, J. Am. Chem. Soc. 115 (1993) 2731.
[13] R. Sanchez-Delgado, D. Rondón, A. Andriollo, V. Herrera, G. Martín, B. Chaudret, Organometallics 12 (1993) 4291.
[14] R. Sánchez-Delgado, V. Herrera, L. Rincón, A. Andriollo, G. Martín, Organometallics 13 (1994) 553.
[15] C. Bianchini, A. Meli, M. Peruzzini, F. Vizza, S. Moneti, V. Herrera, R. Sánchez-Delgado, J. Am. Chem. Soc. 116 (1994) 4370.
[16] C. Bianchini, V. Jimenez, A. Meli, F. Vizza, V. Herrera, R. Sánchez-Delgado, Organometallics 14 (1995) 2342.
[17] V. Herrera, A. Fuentes, M. Rosales, R. Sánchez-Delgado, C. Bianchini, A. Meli, F. Vizza, Organometallics 16 (1997) 2465.
[18] K. Taguchi, F. Westheimer, J. Org. Chem. 36 (1971) 1570.
[19] J.L. Herde, J.C. Lambert, C.V. Senoff, Inorg. Synth. 15 (1974) 18.
[20] L.M. Haines, E. Singleton, J. Chem. Soc., Dalton Trans. (1972) 1891.
[21] J. Chatt, L.M. Venanzi, J. Chem. Soc. (London) 4 (1957) 4735.
[22] R. Schrock, J.A. Osborn, J. Am. Chem. Soc. 93 (1971) 2397.
[23] R.H. Crabtree, P.C. Demou, D. Eden, J.M. Mihelcic, C.A. Parnell, J.M. Quirk, G.E. Morris, J. Am. Chem. Soc. 104 (1982) 6994.
[24] IUPAC, Solubility DATA Series: Hydrogen and Deuterium, Vol. 5/6, p. 219